

# Investigation of the haemodynamic environment of bifurcation plaques within the left coronary artery in realistic patient models based on CT images

Thanapong Chaichana · Zhonghua Sun · James Jewkes

Received: 17 November 2011 / Accepted: 31 March 2012 / Published online: 17 April 2012  
© Australasian College of Physical Scientists and Engineers in Medicine 2012

**Abstract** The aim of this study was to investigate the plaques at the left coronary artery (LCA) and their effect on the haemodynamic and wall shear stress (WSS) in realistic patient models. Three sample patients with left coronary disease were selected based on CT data. The plaques were present at the left anterior descending and left circumflex branches with more than 50 % lumen narrowing. Computational fluid dynamics analysis was used to perform simulation of patient-specific models with realistic physiological conditions that demonstrate in vivo cardiac flow. WSS and blood flow in the LCA were measured during cardiac cycles. Our results showed that WSS was found to increase at the stenotic locations and decrease at pre- and post-plaque locations, whilst the recirculation location was found at post-plaque regions. There is a strong correlation between coronary bifurcation plaques and hemodynamic and WSS changes, based on the realistic coronary disease models.

**Keywords** Atherosclerosis · Haemodynamic · Computational fluid dynamics · Coronary artery disease · Plaques

## Introduction

Computed tomography (CT), a non-invasive medical imaging modality, is increasingly used to diagnose coronary artery disease (CAD), in particular, the evaluation of coronary plaques with regard to their effect on a patient's prognosis [1, 2]. The emergence of multislice coronary computed tomography angiography (CCTA) and the latest CT scanners, has enabled CAD, and coronary plaque detection with high diagnostic accuracy [1, 2]. However, it is limited to the anatomical details and is unable to provide the haemodynamic changes in the coronary artery due to the presence of plaques. The CCTA has been used to characterise the different compositions of coronary plaques, with similar diagnostic value when compared to intravascular ultrasound [3]. Computational fluid dynamics (CFD) has overcome the limitations of CT imaging, and previous studies have used CFD to analyse the haemodynamic parameters in reconstructed coronary arteries, to indicate a plaque's progression [4, 5].

Haemodynamic variation is an important factor which influences the change of static pressure and wall shear stress (WSS) in the artery, thus enabling the investigation of the development of atherosclerotic plaques [6–8]. Coronary plaques are generally formed at bifurcation locations, as confirmed by previous studies [6–11]. The plaques commonly form at the left anterior descending (LAD) and left circumflex (LCX) [9, 12] and lead to the lumen narrowing with at least 50 % stenosis, inducing myocardial ischemic changes [7, 13]. Therefore, the study of the local blood flow changes due to plaques at left coronary bifurcation in realistic vascular geometry can provide an improved understanding of their effect. The purpose of this study was to investigate the corresponding influence of plaques on hemodynamic variations at coronary bifurcations, with specific patients in CAD.

T. Chaichana · Z. Sun (✉)  
Discipline of Medical Imaging, Department of Imaging and Applied Physics, Curtin University, GPO Box U1987, Perth, WA 6845, Australia  
e-mail: z.sun@curtin.edu.au

J. Jewkes  
Fluid Dynamics Research Group, Department of Mechanical Engineering, Curtin University, Perth, WA 6845, Australia

## Materials and methods

### Patient data selection

Three patients with suspected CAD underwent multi-slice coronary CT angiography and were selected for this study, based on CT findings. CT data was processed to reconstruct the 3D left coronary artery (LCA) models. All patients had clinical symptoms of typical chest pain and a history of hypertension. Coronary CT angiography showed significant lumen stenosis caused by plaques in the LCA and its branches. The patient demographics are shown Table 1. At

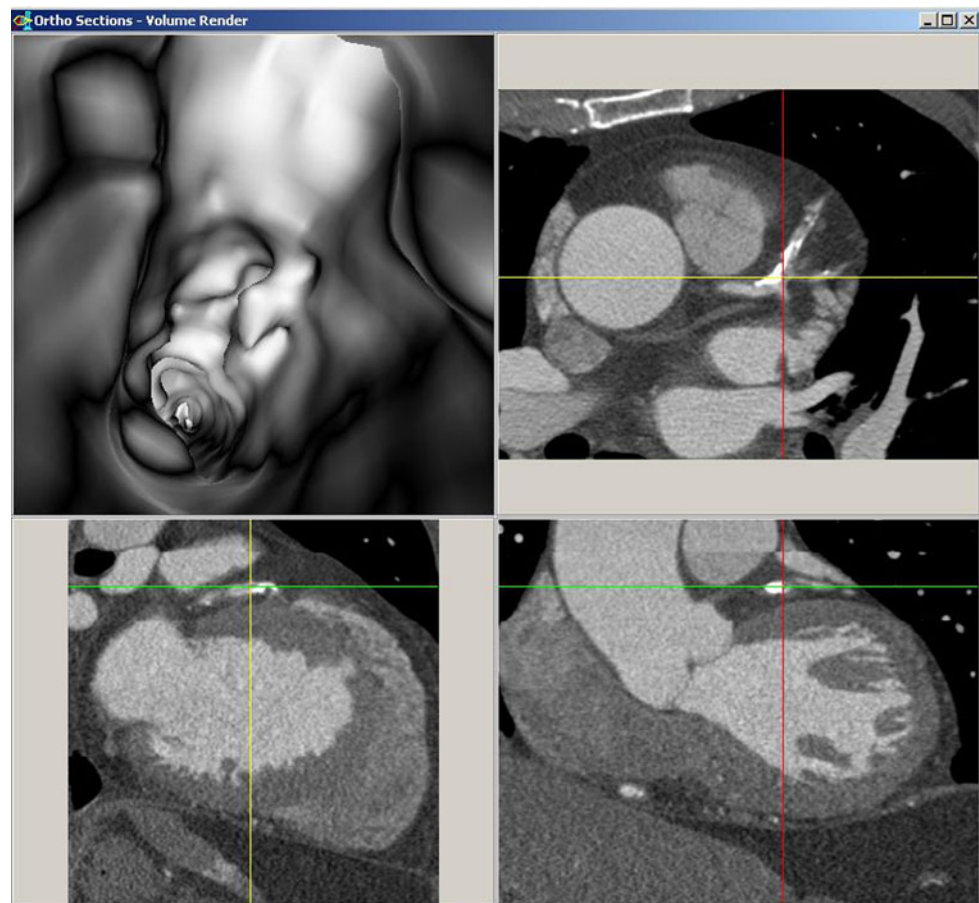
**Table 1** Patient characteristics in three selected patients with suspected CAD

No.	Age (years)	Sex	Degree of coronary stenosis due to plaques		Left bifurcation angle (°)
			LAD (%)	LCX (%)	
A	55	Male	>50	>50	95
B	59	Female	>70	>50	133
C	52	Male	>50	<50	140

least 60 % lumen stenosis was noticed at the LAD and LCX, since more than 50 % lumen narrowing leads to significant blood flow variations within the CAD [7]. The original sample patient's volume CT data was collected in "DICOM format". The calcified plaque-locations were analysed with use of a 3D visualisation tool, virtual intra-vascular endoscopy (VIE), to visualise the stenosis lumen in the sample specific-patients as shown in Fig. 1. The commercial biomedical imaging software Analyze 7.0 (Analyze Direct, Inc., Lexana, KS, USA) was used to identify plaque locations at the bifurcations, and segment the LCA and its branches. These medical imaging techniques were applied to generate 3D LCA models with object-map creations, manual hand editing, and segmented post-processing techniques, with details having been described in previous studies [14, 15]. The 3D LCA surfaces were created, consisting of left main stem (LMS), LAD, LCX and its side-branches. The 3D LCA surfaces were saved in "Binary STL format" for generation of the computational models.

In summary, four plaques were simulated in these three selected patients, with two plaques simulated in the LAD and LCX in patient 1, one plaque in the LAD in patient 2,

**Fig. 1** CT VIE imaging was generated to identify the calcified plaque locations at the bifurcation in the LCA (*top left* image). Extensive calcified plaque is demonstrated at the LAD on 2D axial (*top right* image), and coronal and sagittal views (*bottom left* and *right* images)



and another plaque in the left bifurcation in the remaining patient.

#### Computational left coronary and plaques modelling

Patient's binary STL files were transferred to computer workstation, and Blender version 2.48 (Blender Institute, Amsterdam, the Netherlands) was used for reconstruction purposes. The LCA surfaces were gently smoothed to reduce any non-physical artefacts caused by sharp edges. Patient's surface models were kept to the original rough surface geometry, however unwanted anatomical structures (such as bones, soft tissues) and digital artefacts were removed. The computational LCA models that were used in this study are shown in Fig. 2. LCA models were saved into "STL format" for mesh generation. ANSYS ICEM CFD version 12 (ANSYS, Inc., Canonsburg, PA, USA) was used to generate the computational elements of the study models (details having been described in previous studies [6, 16, 17]). The LCA models were configured with a hexahedral mesh of  $\sim 1 \times 10^6$  nodes and  $9 \times 10^5$  elements, while the plaque-sections were configured with a tetrahedral mesh of around  $1.5 \times 10^4$  nodes and  $7.8 \times 10^4$  elements. Meshing models were saved in 'GTM format' for computation of haemodynamic analysis.

#### Computational hemodynamic analysis

A time dependent simulation was computed, using realistic physiological boundary conditions to model the actual in

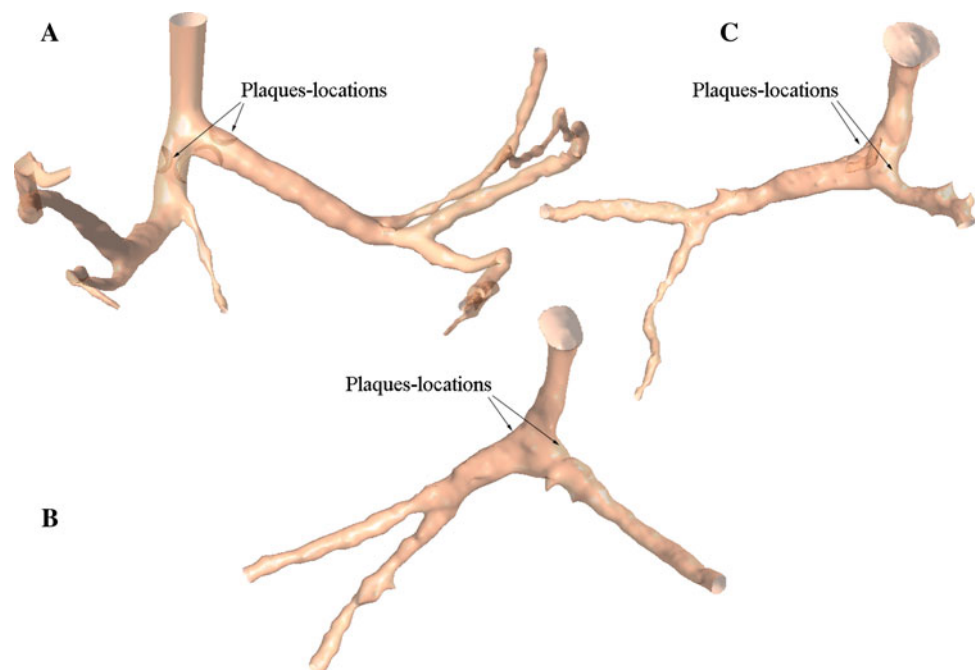
vivo conditions. The accurate boundary conditions of pulsatile flow velocity and pressure were calculated based on Fourier series equations, reconstructed from pulsatile graphs taken from McDonald's Blood Flow in Arteries [18] using Matlab (MathWorks, Inc. Natick, MA, USA). The velocity and pressure profiles were applied at the main inlet (LMS) and outlets (LAD and LCX), respectively, for all study LCA models [6]. Rheological properties were applied with a blood density of  $1,060 \text{ kg/m}^3$ , blood viscosity of  $0.0035 \text{ Pa s}$  [19, 20] and plaque was assumed to be a rigid body [21]. No-slip conditions were applied at the coronary walls, and blood was assumed to be Newtonian. Blood flow was assumed to be laminar and incompressible [22]. ANSYS CFX version 12 (ANSYS, Inc., Canonsburg, PA, USA) was used to solved the Navier–Stokes equations by  $\sim 100$  iterations per time-step within 1.0 s of pulsatile flow and pressure (1 time-step is representing 0.0125 s). A converged solution was obtained for a residual target of less than  $0.1 \times 10^{-3}$ , and the computational time consumption was roughly 2 h for each study case. The hemodynamic profiles and WSS were calculated and visualised using ANSYS CFD-Post version 12 (ANSYS, Inc.).

#### Results

##### Effect of plaques on blood flow at the left coronary bifurcation

The current study was performed based on in vivo physiological conditions during cardiac cycles. The

**Fig. 2** The reconstructed patient-specific left coronary models have been used in this analysis and these models correspond to the patients in Table 1



peak systolic and mid diastolic phases were indicated at the time of 0.4 and 0.7 s, respectively. The results of this simulation show the influence of bifurcation plaques located at the LAD and LCX branches on hemodynamic changes. Figure 3 demonstrates the plaque's effect on flow velocity patterns at the left bifurcation. The 10 coloured levels were used to show the velocity values which ranged from 0 to 30.5 mm/s. The LCA model with patient's diseased bifurcation plaques demonstrated a significant increase of flow velocity at the plaque locations, which ranged from 27.11 to 30.5 mm/s (peak systolic) and 23.72 to 27.11 mm/s (mid diastolic, not shown). Highest velocity was reached at LAD and LCX branches where coronary plaques resulted in significant lumen narrowing. The recirculating regions were found at post-plaque locations in the LAD and LCX (Fig. 3).

**Fig. 3** Visualisation of velocity streamlines of Patient 'A' with presence of coronary plaques (a) and without plaques (b) during the systolic peak of 0.4 s. *Arrows* indicate the regions of low flow velocity which occurred at pre- and post-plaque positions. *Double arrows* reveal the regions of high flow velocity

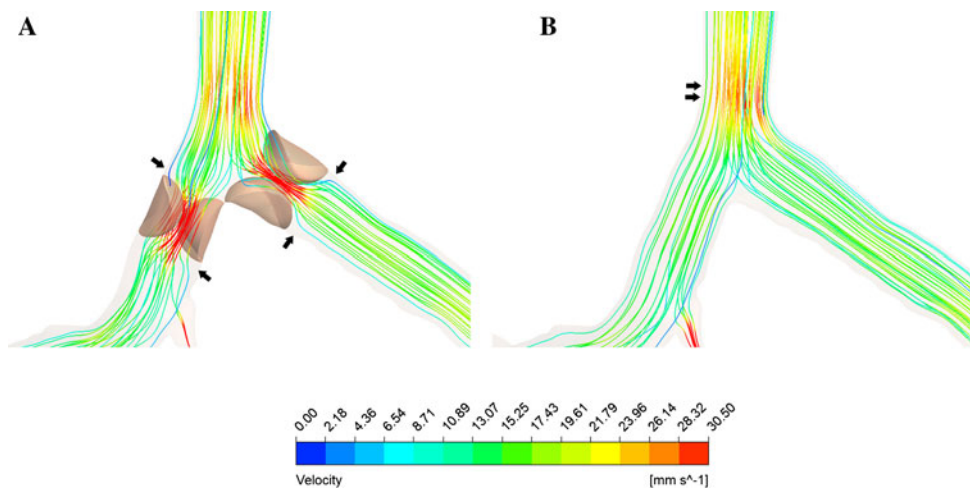
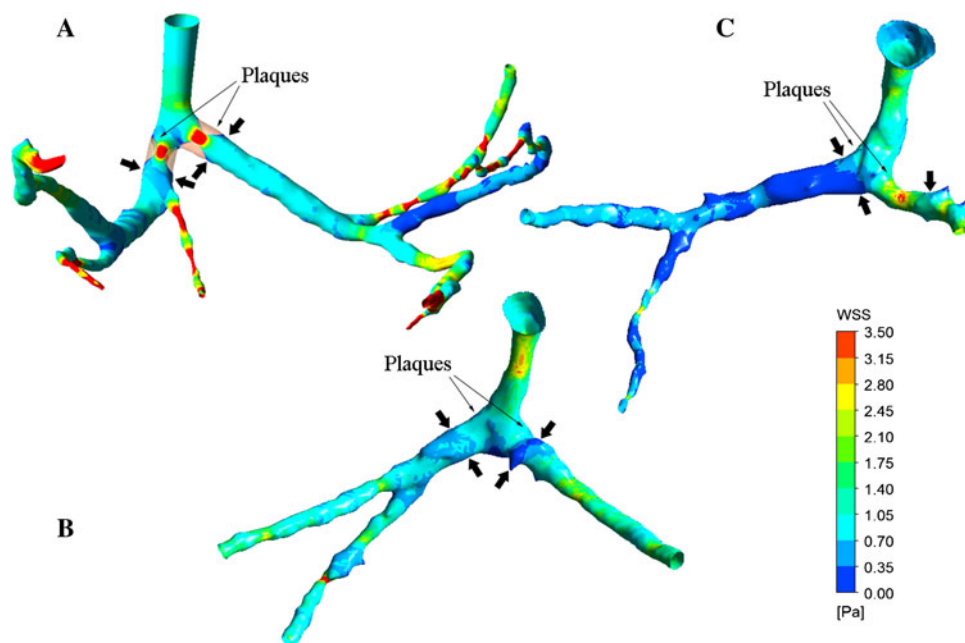


**Fig. 4** Visualisation of WSS of the three patients with the coronary plaques condition during the systolic peak of 0.4 s. *Arrows* indicate the regions of low WSS which occurred at pre- and post-plaque positions



## Effect of plaques on WSS at the left coronary bifurcation

Calculated WSS was visualised at the velocity peak of the systolic and diastolic phases, as shown in Fig. 4. The contour of 10 coloured scales was used to show the WSS values, which ranged from 0 to 3.50 Pa (Fig. 4). WSS distributions in all three patients were similar, with high WSS values ranging from 3.15 to 3.50 Pa at the plaque locations (Fig. 4). Low WSS was found at pre- and post-plaque locations (values ranged from 0 to 0.70 Pa).

## Discussion

This study shows that bifurcation plaques can produce significant haemodynamic effects on blood flow and WSS

changes in realistic patient-specific models of the LCA. The results of this study provide a clinical understanding of coronary plaques with regard to their subsequent effect on blood flow, which could lead to the worsening of atherosclerosis. Plaques are usually located at the bifurcated regions, and early studies have shown that plaques form at the coronary bifurcation [6–12]. The current medical imaging modality of CT is limited to anatomical details, but fails to analyse the haemodynamic and WSS changes [1–3, 9]. Computational analysis of reconstructed coronary vessels is available to detect blood flow and WSS changes in the restricted conditions of modern imaging diagnosis [6, 16, 17].

This study investigated two main areas: flow velocity and WSS, and quantified the effects of bifurcation plaques on haemodynamic factors in patient-specific LCA models. Selected patient's artery geometry was reconstructed to generate the LCA models with significant lumen stenosis. High WSS regions (Fig. 4) were found at the stenotic locations and this seems to indicate that the potential plaques may rupture at high WSS locations [23]. Low WSS locations (Fig. 4) were found at pre- and post- plaque locations, these causes may lead to the progression of plaques [6–8]. Flow velocity was increased at stenotic locations, and recirculating flow was displayed at post-plaque locations (as shown in Fig. 3). According to the haemodynamic analysis, the plaques tend to develop at post-plaque locations, in low flow velocity, recirculating regions [6–8]. Our investigation provides an insight into the effect of bifurcation plaques at LAD and LCX branches on the haemodynamic parameters and demonstrates the subsequent haemodynamics surrounding plaque locations.

Recent studies have presented clinical data regarding the distribution of high-risk plaques in human coronary arteries [24, 25] and focal development of atherosclerosis was related to the plaque configuration in the bifurcation regions. It has been shown that the stenoses in left coronary bifurcations may cause haemodynamic and WSS variations to the main coronary arteries and their side-branches [26, 27]. The role of WSS distribution is associated with plaque progression, and a region of high WSS has been considered contributing to the rupture and thrombosis in atherosclerotic plaques, while the location of low WSS may lead to developed progression of plaque area [28]. Our results are in line with these reports as we noticed the high WSS at the stenotic positions and low WSS at the pre- and post-plaque conditions. These findings are valuable for improving understanding of the effects of plaques, and consequently the mechanisms underlying the development of atherosclerosis.

Patient-specific LCA models of CFD analysis have some limitations that should be addressed. The simulation did not consider the elasticity of the coronary wall. The surface of the stenoses was assumed to be smooth and this

assumption has been shown to be reasonable in this case [26]. Furthermore, the assumption of a non-Newtonian viscosity can be important in low flow areas. However, assumption of a rigid coronary wall is reasonable in this configuration [22]. Furthermore, patient-specific LCA models were limited as only three patients were included in this study. It is possible that plaques only occur at one side of the coronary artery, resulting in stenosis. Future studies with inclusion of more coronary models with different configurations based on a more realistic idealized geometry should be performed.

In conclusion, we performed a computational analysis of bifurcation plaques in the realistic LCA with coronary disease, at bifurcation locations between LAD and LCX. There is a direct influence of bifurcation plaques in the LCA on haemodynamic and WSS changes, such as recirculating flow, low flow velocity regions, and high WSS, indicating the potential risk for plaques to rupture. Further studies focusing on the larger populations of patient-specific left coronary disease should be performed to verify our results.

## References

1. Sun Z, Dimpudus FJ, Nugroho J, Adipranoto JD (2010) CT virtual intravascular endoscopy assessment of coronary artery plaques: a preliminary study. *Eur J Radiol* 75:e112–e119
2. Australian Institute of Health and Welfare (2006) Australia's health 2006. AIHW, Canberra
3. Feuchtner GM, Cury RC, Jodocy D, Friedrich GJ, Blumenthal RS, Budoff MJ, Nasir K (2011) Differences in coronary plaques composition by noninvasive computed tomography in individuals with and without obstructive coronary artery disease. *Atherosclerosis* 215:90–95
4. Ribicki FJ, Melchionna S, Mitsouras D, Coskun AU, Whitmore AG, Steigner M, Nallamshetty L, Welt FG, Bernaschi M, Borkin M, Sircar J, Kaxiras E, Succi S, Stone PH, Feldman CL (2009) Prediction of coronary artery plaque progression and potential rupture from 320-detector row prospectively ECG-gated single heart beat CT angiography: Lattice Boltzmann evaluation of endothelial shear stress. *Int J Cardiovasc Imaging* 25:289–299
5. Shanmugavelayudam SK, Rubenstein DA, Yin W (2010) Effect of geometrical assumptions on numerical modelling of coronary blood flow under normal and disease conditions. *ASME J Biomech Eng* 132:061004
6. Chaichana T, Sun Z, Jewkes J (2011) Computation of hemodynamics in the left coronary artery with variable angulations. *J Biomech* 44:1869–1878
7. Fuster V (1994) Lewis A. Conner memorial lecture. Mechanisms leading to myocardial infarction: insights from studies of vascular biology. *Circulation* 90:2126–2146
8. Asakura T, Karino T (1990) Flow patterns and spatial distribution of atherosclerotic lesions in human coronary arteries. *Circ Res* 66:1045–1066
9. Sun Z, Cao Y (2011) Multislice CT angiography assessment of left coronary artery: correlation between bifurcation angle and dimensions and development of coronary artery disease. *Eur J Radiol* 79:e90–e95

10. Han SH, Puma J, Garcia-Garcia HM, Nasu K, Margolis P, Leon MB, Lerman A (2010) Tissue characterisation of atherosclerotic plaque in coronary artery bifurcations: an intravascular ultrasound radiofrequency data analysis in humans. *EuroIntervention* 6:313–320
11. Gziut AI (2006) Comparative analysis of atherosclerotic plaque distribution in the left main coronary artery and proximal segments of left anterior descending and left circumflex arteries in patients qualified for percutaneous coronary angioplasty. *Ann Acad Med Stetin* 52:51–62
12. Kimura BJ, Russo RJ, Bhargava V, McDaniel MB, Peterson KL, DeMaria AN (1996) Atheroma morphology and distribution in proximal left anterior descending coronary artery: in vivo observations. *J Am Coll Cardiol* 27:825–831
13. Cho GY, Lee CW, Hong MK, Kim JJ, Park SW, Park SJ (2001) Effects of stent design on side branch occlusion after coronary stent placement. *Catheter Cardiovasc Interv* 52:18–23
14. Sun Z, Winder RJ, Kelly BE, Ellis PK, Hirst DG (2003) CT virtual intravascular endoscopy of abdominal aortic aneurysms treated with suprarenal endovascular stent grafting. *Abdom Imaging* 28:80–87
15. Sun Z, Winder RJ, Kelly BE, Ellis PK, Kennedy PT, Hirst DG (2004) Diagnostic value of CT virtual intravascular endoscopy in aortic stent grafting. *J Endovasc Ther* 11:3–25
16. Sun Z, Chaichana T (2010) Fenestrated stent graft repair of abdominal aortic aneurysm: hemodynamic analysis of the effect of fenestrated stents on the renal arteries. *Korean J Radiol* 11:95–106
17. Sun Z, Chaichana T (2009) Investigation of the hemodynamic effect of stent wires on renal arteries in patients with abdominal aortic aneurysms treated with suprarenal stent-grafts. *Cardiovasc Intervent Radiol* 32:647–657
18. Nichols W, O'Rourke M (2005) McDonald's blood flow in arteries. Hodder Arnold, London, pp 326–327
19. Boutsianis E, Dave H, Frauenfelder T, Poulikakos D, Wildermuth S, Turina M, Ventikos Y, Zund G (2004) Computational simulation of intracoronary flow based on real coronary geometry. *Eur J Cardiothorac Surg* 26:248–256
20. Milnor W (1989) *Hemodynamics*. Williams & Wilkins, Baltimore
21. Sun Z, Mwilpatayi B, Chaichana T, Ng C (2009) Hemodynamic effect of calcified plaque on blood flow in carotid artery disease: a preliminary study. *IEEE Proc Bio Biomed Eng* 1:1–4
22. Johnston BM, Johnston PR, Corney S, Kilpatrick D (2004) Non-Newtonian blood flow in human right coronary arteries: steady state simulations. *J Biomech* 37:709–720
23. Slager CJ, Wentzel JJ, Gijsen FJH, Thury A, van der Wal AC, Schaar JA, Serruys PW (2004) The role of shear stress in the destabilization of vulnerable plaques and related therapeutic implications. *Nat Clin Prac Cardiovasc Med* 2:456–464
24. Cheruvu PK, Finn AV, Gardner C, Caplan J, Goldstein J, Stone GW, Virmani R, Muller JE (2011) Frequency and distribution of thin-cap fibroatheroma and ruptured plaques in human coronary arteries: a pathologic study. *J Am Coll Cardiol* 50:940–949
25. Diletti R, Onuma Y, Farooq V, Gomez-Lara J, Brugaletta S, van Geuns RJ, Regar E, de Bruyne B, Dudek D, Thuesen L, Chevalier B, McClean D, Windecker S, Whitbourn R, Smits P, Koolen J, Meredith I, Li D, Veldhof S, Rapoza R, Garcia-Garcia HM, Ormiston JA, Serruys PW (2011) 6-Month clinical outcomes following implantation of the bioresorbable everolimus-eluting vascular scaffold in vessels smaller or larger than 2.5 mm. *J Am Coll Cardiol* 58:258–264
26. Chaichana T, Sun Z, Jewkes J (2012) Impact of plaques in the left coronary artery on wall shear stress and pressure gradient in coronary side branches. *Comput Methods Biomech Biomed Eng*. doi:10.1080/10255842.2012.671308
27. Chaichana T, Sun Z, Jewkes J (2012) Computational fluid dynamics analysis of the effect of plaques in the left coronary artery. *Comput Math Methods Med* 2012:504367
28. Samady H, Eshtehardi P, McDaniel MC, Suo J, Dhawan SS, Maynard C, Timmins LH, Quyyumi AA, Giddens DP (2011) Coronary artery wall shear stress is associated with progression and transformation of atherosclerotic plaque and arterial remodeling in patients with coronary artery disease. *Circulation* 124:779–788